Evaluation of nonunion fractures in dogs by use of B-mode ultrasonography, power Doppler ultrasonography, radiography, and histologic examination

Marije Risselada, DVM; Henri van Bree, DVM, PhD; Martin Kramer, DVM, PhD; Koen Chiers, DVM, PhD; Luc Duchateau, PhD; Piet Verleyen, DVM; Jimmy H. Saunders, DVM, PhD

Objective—To investigate the use of ultrasonography to assess nonunion of fractures in dogs and to compare results of ultrasonography, radiography, and histologic examination.

Sample Population—8 nonunion fractures in 6 dogs (1 each in 5 dogs and 3 in 1 dog); dogs ranged from 7 to 94 months of age and weighed 6 to 30 kg.

Procedures—Diagnostic assessment consisted of complete clinical and orthopedic examinations, radiography, B-mode (brightness mode) ultrasonography, and power Doppler ultrasonography. Biopsy samples were obtained during surgery for histologic examination. They were stained with H&E and immunolabeled by use of anti-CD31 antibodies. Correlations of power Doppler score, power Doppler count, vessel area, and radiographic prediction with the mean number of vessels counted per hpf were derived.

Results—Radiographically, 7 of 8 nonunion fractures were diagnosed as atrophic and were therefore estimated to be nonviable. Vascularity of nonunion fractures during power Doppler ultrasonography ranged from nonvascularized to highly vascularized. Absolute vessel count during histologic examination ranged from 0 to 63 vessels/hpf; 5 nonunion sites had a mean count of > 10 vessels/hpf. Vascularity during power Doppler ultrasonography was highly correlated with the number of vessels per hpf, whereas the correlation between the radiographic assessment and histologic evaluation was low.

Conclusions and Clinical Relevance—Radiographic prediction of the viability of nonunion fractures underestimated the histologically assessed vascularity of the tissue. Power Doppler ultrasonography provided a more accurate estimation of the viability of the tissue and therefore the necessity for debridement and autografts during revision surgery. (*Am J Vet Res* 2006;67:1354–1361)

Abbreviations

CT	Computed tomography
MRI	Magnetic resonance imaging

Complications can arise during fracture healing. These can include infections, hyperemia, ischemia, and avascular necrosis, all of which can lead to delayed union or nonunion. Nonunion can also be caused by instable immobilization and excessive distraction or compression.[1] Nonunion fractures are those in which healing has ceased, whereas delayed union fractures are those in which healing requires longer than expected.[2,3]

Early recognition of complications is important to enable clinicians to take immediate corrective actions. Clinical characteristics of delayed union or nonunion fractures include lack of rigidity, crepitation, abnormal movement in the fracture region, signs of pain during manipulation of the fracture region, inability or unwillingness to bear weight, deformity of the limb, disuse atrophy of the limb, and an abnormal callus (profuse or total lack of a callus).[1,3,4]

Classically, nonunion fractures have been delineated into viable and nonviable categories. Viable nonunion fractures are described as hypertrophic, slightly hypertrophic, and oligotrophic. All are caused by instability. Nonviable nonunion fractures have an interruption of the blood supply and are classified as dystrophic, necrotic, defect, and atrophic.[1]

Radiography is the imaging method traditionally used for the assessment of fracture healing. The main radiographic signs of nonunion include a visible fracture gap, clearly defined fracture ends, obliteration of the marrow cavity, and a callus (if evident) that does not bridge the fracture gap.[2] Classification into viable and nonviable categories is based primarily on whether there is a callus. In hypertrophic viable nonunion fractures, abundant callus formation is visible but the callus does not bridge the fracture gap. Fractures with evidence of a small amount of nonbridging callus have been termed slightly hypertrophic[1] but are also classified as viable. In atrophic nonunion fractures, minimal or no callus formation is evident.[1,2,4] There is less uniformity in the appearance of the fracture ends, other than the amount of callus formation. According to 1 source,[2] sclerotic ends are an indication for a nonviable nonunion fracture. However, another author[4] believes that sclerotic ends should be classified as viable and sharp tapered ends classified as nonviable. This illustrates the difficulty that exists when radiography is used to predict the type of nonunion.

Received December 13, 2005.
Accepted February 10, 2006.
From the Departments of Medical Imaging of Domestic Animals (Risselada, van Bree, Kramer, Verleyen, Saunders), Pathology, Bacteriology and Poultry Diseases (Chiers), and Physiology, Biochemistry, and Biometrics (Duchateau), Faculty of Veterinary Medicine, Ghent University, Salisburylaan 133, B-9820 Merelbeke, Belgium. Dr. Kramer's present address is the Klinik für Kleintiere, Chirurgie, Fachbereich Veterinärmedizin, Justus-Liebig-Universität Giessen, Frankfurter Straße 108, D-35392 Giessen, Germany.
Address correspondence to Dr. Risselada.

Classification into nonviable and viable is necessary for determining a plan of treatment because debridement is necessary for nonviable nonunion fractures, whereas rigid immobilization (with or without autograft placement) is used for viable nonunion fractures. However, authors in 1 study[5] reported that induced atrophic nonunion fractures in rabbits were vascularized. Therefore, assessment of vascularization, rather than estimating the vascular supply, may be more useful in radiographic evaluation of the type of nonunion fracture.

Scintigraphy has been used to examine vascularization of nonunion fractures[6] and in an attempt to predict the development of nonunions.[7] Venous osseography has also been evaluated experimentally to test the validity of the method for use in assessing vascularization of fractures.[8] However, it would require that an animal be sedated or anesthetized to perform scintigraphy and venous osseography, which would make them less desirable options.

Investigators have used CT to reconstruct a multiplanar image of a nonunion site,[9] and MRI has been used to predict the development of delayed union in a group of 12 patients, 5 of which had a delayed union.[10] In that report, differences were visible between images obtained from normally healing fractures and those that developed delayed union at 3 to 6 weeks after the trauma. However, CT and MRI are not yet universally available in veterinary medicine. Furthermore, CT and MRI cannot be used on surgically treated fractures because implants will create numerous artefacts. Additionally, it would require that an animal be anesthetized to perform CT or MRI procedures.

Ultrasonographic images of delayed unions and nonunion fractures in humans have been reported.[11,12] A lack of developing callus in the fracture gap, with an initial increase in nonhomogenicity and a subsequent increase in hyperechogenicity, is an early indication of delayed union.[11] In another report,[12] investigators describe nonunion as a lack of a bony bridge consisting of several bony fragments with poor alignment or a structure with an extreme nonhomogeneous tissue echogenicity.

In addition, B-mode (brightness mode) ultrasonography has been used to classify the types of nonunion fractures. Hypertrophic and atrophic nonunion fractures both have characteristic ultrasonographic features. Hypertrophic nonunion fractures will be visible as structures with a hypoechoic to anechoic, nonhomogeneous tissue echogenicity filling the fracture gap with no progression to hyperechogenicity over time. No callus formation is visible in atrophic nonunions. Also, an image with rounded, extremely smooth bony edges is indicative of atrophic nonunion.[11]

Laser Doppler ultrasonography has been used to assess the viability of bone fragments,[13] and color Doppler[14] and power Doppler[15] ultrasonography have been used to assess fracture healing. Our hypothesis for the study reported here was that power Doppler ultrasonography would be a better modality than radiography to assess vascularization of nonunion fractures in dogs. Histologic evaluation was used to assist in comparison of the imaging techniques.

Materials and Methods

Animals—Six client-owned dogs were used in the study. The dogs were clinical patients at our university facility. Five dogs each had a single nonunion fracture, whereas the other dog had 3 nonunion fractures. A nonunion fracture was defined as lack of progression in healing during a period of 6 weeks or failure to heal after 5 months. Written owner consent regarding the surgery was obtained prior to surgical interventions. All included animals were clinical patients that were treated in accordance with the current standards of surgical and postoperative care. No research animals were included, nor were surgical interventions performed solely for the purpose of this study.

Procedure—For all dogs, evaluation of craniocaudal and mediolateral radiographs and B-mode and power Doppler ultrasonography were part of the diagnostic examination. Radiographs were obtained by use of equipment with a range of 40 to 125 kV and 0.5 to 500 mAs[a] or equipment with a range of 40 to 110 kV and 0.2 to 130 mAs.[b] A linear transducer was used to perform B-mode ultrasonography.[c] Power Doppler ultrasonography was performed by use of a setting of 6.7 MHz, pulse-repetition frequency of 1.3 kHz, and a wall filter of 102 Hz.

Ultrasonography—Hair was clipped over the region of interest, and coupling gel[d] was applied to the skin. One or 2 assistants were required to aid in positioning of the dogs on the table. None of the dogs was sedated for the ultrasonographic examinations. Ultrasonographic examinations were performed by use of standard planes and techniques.[16]

All ultrasonographic examinations were assessed by a single investigator (MR). The Doppler signal was scored (scale of 0 to 3) for each of 3 variables (color coding, number of signals, and vessel area; **Appendix**).[15] Measurements were obtained from images that were saved during 1 session. A mechanical callipers was used to measure vessel area, and compensation for enlargement was accomplished by use of the calibrated scale on each saved image. In situations in which there was no evidence of the power Doppler signals, only 1 still image was saved. In situations in which there were power Doppler signals for evaluation, multiple still images were saved. Thus, 1 to 5 still images/nonunion site were used for measurements, and the mean score was calculated. The mean score was multiplied by 10 to yield scores within the same range and enable comparison with the vessel counts for the histologic examinations.

Radiography—Radiographs were assessed by a board-certified veterinary radiologist, 2 board-certified veterinary surgeons, a clinician who was board-certified in both veterinary radiology and veterinary surgery, a veterinarian who was in the final year of a residency in veterinary radiology, and a staff veterinary orthopedic surgeon. Assessments were performed in accordance with criteria described in a textbook.[4] Investigators were not aware of results of histologic or ultrasonographic examinations or any preceding radiographic diagnoses. Criteria used to determine a diagnosis for the type of nonunion were based on the detection of a callus and the amount of callus. Abundant nonbridging callus was diagnosed as a hypertrophic, viable nonunion.[1,2,4] A small amount of callus was classified as a slightly hypertrophic viable nonunion, and a lack of callus with atrophied ends was classified as an atrophic nonviable nonunion.

Histologic examination—Biopsy specimens were obtained during surgery. Samples were obtained from both bone ends at the nonunion sites. Biopsy specimens were immediately immersed in phosphate-buffered formaldehyde solution (4%), embedded in paraffin, and processed for sec-

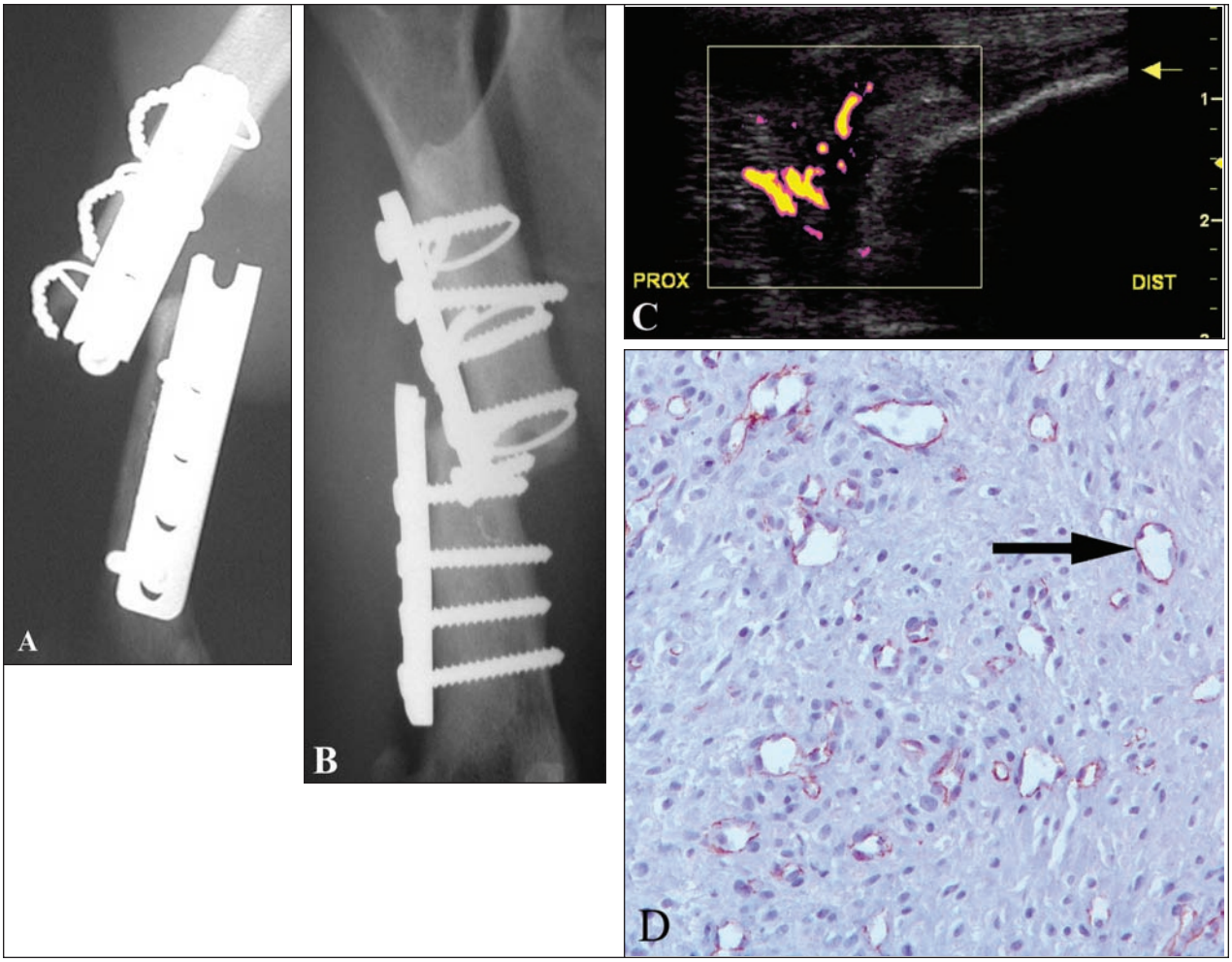

Figure 1—Lateral (A) and craniocaudal (B) radiographic views, longitudinal power Doppler image (C), and photomicrograph of a section of tissue (D) obtained from the right femur of a dog with a vascularized nonunion fracture. A 9-hole plate (broken through the fifth hole) is visible on the lateral cortex, and 3 cerclage wires are visible on the proximal segment. The distal end of the femur is displaced caudolaterally. No new bone formation is visible at the fracture site. In panel C, the power Doppler image was obtained by use of a lateral approach. Notice that the proximal (PROX) and distal (DIST) directions are indicated. The proximal segment of the bony surface is not visible, and the ends of the distal segment are irregular (yellow arrow). Three large, intense, power Doppler signals and several smaller ones are evident on the ultrasonogram. In the power Doppler window, abundant signals are visible in tissues with a nonhomogeneous hypoechoic to anechoic image, representing the fracture gap. Marks on the right side are at intervals of 1 cm. In panel D, CD31 antibodies were used to immunolabel tissue to enhance visibility of blood vessels at the nonunion site. Abundant vascularization (endothelial lined cavities) is evident (black arrow).

tioning in accordance with standard techniques. Sections (5 µm thick) were stained with H&E. The sections of the ulna and radius containing the 3 nonunion sites from the same dog were decalcified prior to staining with H&E. To highlight vessels, endothelial cells were immunolabelled by use of monoclonal mouse anti-human CD31 antibodies.[e]

Histologically, the degree of vascularization was measured by use of a semiquantitive method. The number of vessels per hpf (200X magnification) was counted at 2 or 3 representative sites/sample. When several biopsy specimens were obtained from the same nonunion site, counts were performed for each sample and the mean number of vessels per hpf was calculated. For vessels located at the edge of images, we included counts for only 2 of the 4 edges to avoid overestimating the number of vessels.

Statistical analysis—The relationship between the logarithmically transformed number of vessels determined during histologic examination of biopsy specimens and values for 3 Doppler variables (vessel area, number of vessels, and power Doppler score multiplied by 10) was analyzed by use of linear regression, with the Doppler variables assigned as the response variables. The relationship between the logarithmically transformed number of vessels counted during histologic examination and the number of radiographic assessments characterized as nonviable for the 6 investigators was analyzed by use of a logistic regression model. Furthermore, Spearman rank correlation coefficients[f] were derived between the number of vessels determined during histologic examination and each of the 3 Doppler variables and between the number of vessels determined during histologic examination and the number of radiographic assessments characterized as nonviable. For all analyses, values of $P < 0.05$ were considered significant.

Results

Animals—The 6 dogs ranged from 7 to 94 months of age (mean, 33.7 months; median, 28 months). Body weight ranged from 6 to 30 kg (mean, 17.5 kg; median, 16.4 kg). All dogs were examined because of nonunion fractures. Interval between initial fracture

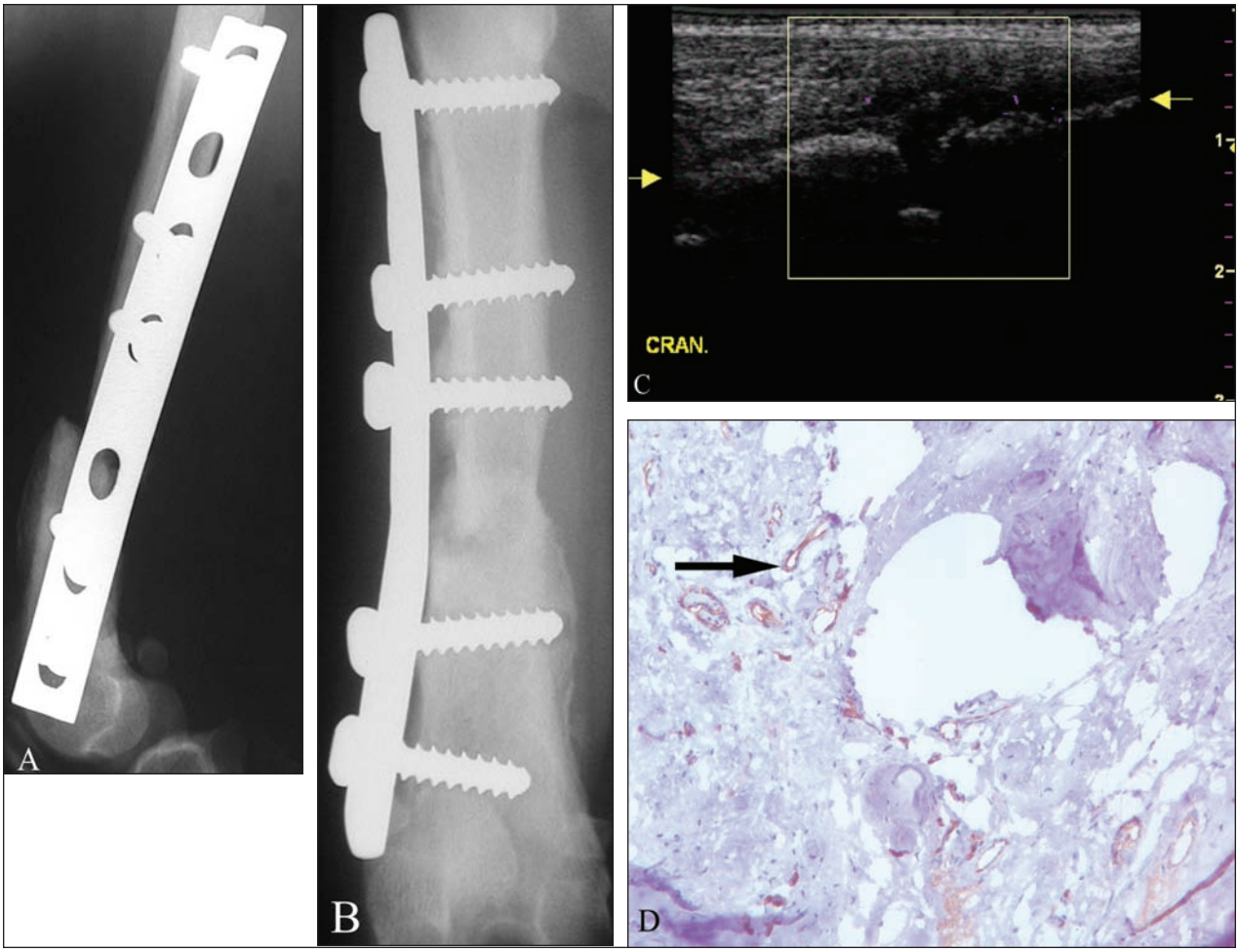

Figure 2—Lateral (A) and craniocaudal (B) radiographic views, longitudinal power Doppler image (C), and photomicrograph of a section of tissue (D) obtained from the right femur of a dog with a nonvascularized nonunion fracture. A 7-hole, 4.5 dynamic compression plate is visible on the lateral cortex of the femur. A radiolucent band separates the plate and bony surface. In panel A, the distal segment of the femur is angled and has a smooth sclerotic appearance. In panel B, new bone formation is visible at the medial cortex of the distal segment but does not extend to the fracture site. In panel C, the power Doppler image was obtained by use of a craniolateral approach cranial to the plate. Notice that the cranial (CRAN) direction is indicated. The bony surface (yellow arrows) is interrupted and has rounded segment ends, and no vascularization is evident in the power Doppler window. In panel D, antiCD31 antibodies were used to immunolabel tissue to enhance visibility of blood vessels at the nonunion site. Only sparse vascularization (endothelial lined cavities) is evident (black arrow).

management and examination at our facility to diagnose nonunion ranged from 3 to 12.5 months (mean, 5.2 months; median, 4.5 months).

Eight nonunion fractures were evaluated. Affected bones were the femur (n = 3), radius (2), ulna (2), and tibia (1). In the dog with 3 nonunion fractures, middiaphyseal fractures of the radius and ulna resulted in nonunion in both bones. In addition, 1 nonunion fracture emanated from the proximal hole used for insertion of a pin to correct the initial fracture of the radius. Initial fracture management ranged from conservative to use of plate osteosynthesis.

After diagnosis of nonunion, management of the dogs consisted of surgery. Owners of the dog with the 3 nonunion fractures opted for amputation of the affected limb. In the other 5 dogs, nonunion fractures were treated by use of cancellous autografts and plate osteosynthesis. All 5 subsequently had complete, uncomplicated healing as assessed by the use of radiography and ultrasonography.

Radiographic assessment—On radiographic examination, 1 nonunion fracture was classified as atrophic nonviable and 1 as hypertrophic viable by all investigators (**Figures 1 and 2**). For the remaining 6 nonunion fractures, most of the investigators diagnosed atrophic nonunions (**Table 1**). There was only periosteal reaction in the caudodistal region of 1 nonunion fracture. Plate failure was evident in 1 nonunion fracture, and screw loosening was evident in all 3 plated nonunion fractures.

Prediction of viability differed vastly among investigators. For predictions made by the 3 radiologists, they agreed for 4 nonunions. The 4 surgeons agreed for 2 nonunions, were evenly divided for 1 nonunion, and had a 3:1 ratio for the remaining 5 nonunions. For the 8 nonunion fractures, correct predictions were made for 2 by the board-certified veterinary radiologist, 3 by a board-certified veterinary surgeon and the clinician board-certified in both veterinary radiology and veterinary surgery, 4 by the other board-certified veterinary

Table 1—Results of radiographic, B-mode ultrasonographic, power Doppler ultrasonographic, and histologic examinations of 8 nonunion fractures in 6 dogs.

	Radiography		B-mode ultrasonography	Power Doppler ultrasonography		Histologic examination	
Bone	**Description**	**Diagnosis***	**Description**	**Doppler score†**	**Doppler signals**	**Vessel count‡**	**Description**
Femur	Sharp, sclerotic ends; no callus visible; displacement caused by plate failure; 2 of 8 screws loose	5 nonviable and 1 viable	Hypoechoic nonhomogenous tissue; large anechoic cavities; 2 cm of displacement; sharp irregular bony ends	2.4	Evident in gap defect, soft tissue, and bony surface	40	Collagen with capillaries and lymphatics
Femur	Sclerotic ends; periosteal proliferation distally; no proliferation proximally (telescoping of ends); radiolucent gap visible; 2 of 5 screws loose	3 nonviable and 3 viable	Hypoechoic, homogenous tissue in discontinuity of cortex (0.5 cm); rounded, smooth bony ends	0	No signal	5	Dense collagenous tissue; lack of mineralization
Femur	Extensive callus with radiolucent areas; gap between bone and plate (half of femoral diameter); 4 of 7 screws loose	6 viable	Mixed anechoic and hypoechoic tissues with small hyperechoic areas; rounded, irregular bone ends	1.9	Evident in gap defect, soft tissue, and bony surface	13	Haphazardly arranged bone formation; cartilaginous metaplasia; bone formation with mineralization; trabecular bone with active osteoblasts and osteoclasts; peripherally vascularized fibrous tissue
Tibia	Oblique nonunion and malunion; sclerosis of ends; rounded caudal ends; sharp cranial ends; callus caudodistally; no callus cranially; no osteosynthesis material	2 nonviable and 4 viable	Discontinuous; filled with hypoechoic tissue; width ranged from 0.3 to 0.5 cm and depth from 0.5 to 1.0 cm (depending on the view); sharp, irregular bone ends	1	Bony surface; not evident in gap defect	13	New bone formation from fibrous tissue and cartilage; area with small vessels; 1 large vessel peripherally
Ulna	Sclerotic ends; no bridging; gap at level of humeroradial joint, probably extending into joint; ununited anconeal process visible; no osteosynthesis material	5 nonviable and 1 viable	Gap of 0.5 cm filled with tissue of homogenous hypoechoic tissue; round, irregular edges	0.7	Evident in gap defect	12	Necrotic bone; highly vascularized cartilaginous matrix peripherally
Radius§	Sclerotic ends; periosteal reaction that did not bridge gap; intramedullary pin in proximal fragment extended to fracture site	4 nonviable and 2 viable	Homogeneous anechoic image, gap of 1 cm and step of 0.5 cm; round, irregular edges	0	No signal	2	Cartilaginous tissue; some areas of mineralization
Radius§,‖	Sclerotic ends; no callus	6 nonviable	Mixed hypoechoic and hyperechoic tissues with anechoic areas; sharp, irregular edges	2	Evident in gap defect, soft tissues, and less on the bony surface	23	Vascularized fibrous tissue
Ulna§	Sclerotic ends; no callus	4 nonviable and 2 viable	Anechoic with some hypoechoic areas; cortex was hypoechoic; irregular, sharp edges	1	Evident in soft tissues but not on the bony surface	9	Peripheral vessels; cartilaginous tissue; some areas of mineralization

*Represents diagnoses for each of the 6 investigators. †Power Doppler ultrasonography score was determined semiquantitatively by use of a scale of 0 to 3 for each of 3 categories (color, vessel area, and number of vessels). ‡Mean number of vessels per hpf. §One of 3 nonunion fractures in the same forelimb of 1 dog. ‖Nonunion fracture that developed from a pinhole created during the initial surgery to repair the fracture.

surgeon and the veterinarian who was in the final year of a residency in veterinary radiology, and 5 by the staff veterinary orthopedic surgeon.

The score assigned most often (median radiographic diagnosis) was used for determination of the correlation coefficient. Odds ratio of a correct diagnosis was 1.21:1. Thus, the probability of a correct radiographic diagnosis (viable or nonviable) increased with the logarithm of the number of vessels in the biopsy specimens, but the odds ratio did not differ significantly (P = 0.48) from 1. Therefore, the diagnoses determined radiographically were independent of the final outcome for degree of vascularization as determined by histologic examination. The correlation coefficient between the median radiographic prediction and histologic examination was 0.29.

B-mode ultrasonography—All B-mode ultrasonographic examinations of tissues in the defect revealed predominantly hypoechoic to anechoic images. Hyperechoic areas were evident in 2 nonunion fractures. These areas were small, irregular, and spread throughout the defect. In 1 nonunion fracture, large anechoic cavities were seen. These probably represented hematomas caused by movement of the femur ends (the plate failed in this fracture).

For 7 nonunion sites, the bone ends had an irregular appearance on B-mode ultrasonography. In 1 nonunion fracture, the proximal and distal bone ends had a rounded, smooth appearance (Table 1). This nonunion fracture had no vascularization evident during power Doppler ultrasonography and a low vessel count (mean, 4.5 vessels/hpf).

Irregular bone ends were rounded in 3 nonunions and sharp in the remaining 5. The 3 nonunions with rounded bone ends had mean power Doppler scores of 0, 0.7, and 1.9 and mean vessel counts of 2, 11.8, and 13 vessels/hpf, respectively. Four of the other 5 nonunions had mean power Doppler scores of 1, 1, 2, and 2.4 and mean vessel counts of 9, 13, 23, and 40 vessels/hpf, respectively.

Power Doppler ultrasonography—Power Doppler signals and scores had large variations. Color scores ranged from 0 to 3. There also was large variation in the number of signals (0 to 12). The number of vessels detected during power Doppler ultrasonography increased significantly (P = 0.013) with the logarithm of the number of vessels detected in the biopsy specimens (mean ± SD slope, 1.98 ± 0.57). The number of vessels detected during power Doppler ultrasonography and number of vessels counted per hpf was highly correlated (r, 0.95). Appearance of the signals and vessel area varied greatly from small, smooth, rounded signals to larger, irregular signals. Range of the total surface area per image was 0.2 to 46.6 mm². There was no significant (r, 0.85; P = 0.10) relationship between vessel area and the logarithm of the number of vessels per hpf (mean slope, 4.82 ± 2.49).

Mean scores for the power Doppler signals ranged from 0 to 2.4. In the nonunion fractures at 2 sites in the radius and various sites in the ulna, scores differed at each site (Table 1). There was a significant (r, 0.95; P = 0.014) relationship between score and the logarithm of the number of vessels per hpf (mean ± SD slope, 6.67 ± 1.94).

High power Doppler scores (1.9 and 2.0, respectively) were found for nonunion fractures with hyperechogenic foci. A score of 0 was found for the nonunion fracture with rounded, smooth bony surfaces.

A qualitative score also was assigned to the regions (bone, defect, and soft tissue) with positive Doppler signals. Scores were divided into nonunion gap, surrounding cortex, and overlying soft tissue. For the nonunion gap, flow signals were found for 4 nonunion fractures. Positive signals were found on the bony surface on 1 side of the gap of 4 nonunion fractures (the proximal segment in 3 nonunions and the distal segment in 1 nonunion). Flow signals were found in the soft tissues of 4 nonunion fractures. In 3 nonunion fractures, signals were found in all 3 areas.

Histologic examination—Histologic examination revealed that the mean vessel count ranged from 2 to 40 vessels/hpf, with a range of 0 to 63 vessels/hpf for the separate counts. Vessel counts differed greatly among nonunion fractures. The 2 sparsely vascularized nonunions had mean vessel counts of 2 and 4.5 vessels/hpf, respectively. The remaining nonunions had vessel counts of 9, 12, 13, 13, 23, and 40 vessels/hpf, respectively. In all nonunions, the main tissue component at the nonunion site was collagenous tissue. In 1 nonunion fracture, necrotic bone was found. The ultrasonographic image in this nonunion was homogeneously hypoechoic. Cartilaginous tissue (cartilage or cartilaginous metaplasia) was found in 5 nonunion fractures. Mineralization was evident in 4 nonunion fractures, but only 2 of these had hyperechoic areas evident during ultrasonography.

Discussion

Diagnosis of a delayed union is necessary to permit early intervention, and knowledge about vascularity is helpful to clinicians who are deciding between surgery and a conservative approach in patients with stable surgical implants. Also, once a nonunion has developed, knowledge about its vascularity is helpful to clinicians who are deciding whether the treatment should consist of providing stability or, alternatively, of debridement, autograft placement, and stabilization.

Typical B-mode ultrasonographic images of hypertrophic and atrophic nonunion types in humans have been described.[11] In that study, investigators found that hypertrophic nonunion fractures will be visible as structures with a hypoechoic to anechoic, nonhomogeneous tissue echogenicity filling the fracture gap with no progression to hyperechogenicity over time. In atrophic nonunion fractures, no callus formation will be visible. In the nonunion fractures of the study reported here, the gap was filled with hypoechogenic or anechogenic tissue, which would suggest an ultrasonographic diagnosis of atrophic nonunion. However, small hyperechoic areas were found in 2 of 8 nonunion fractures, which may suggest a more reactive site than would be expected for an atrophic nonunion.

The only nonunion fracture with smooth bony surfaces evident during ultrasonography was avascular, but a second avascular nonunion fracture had irregular surfaces, so no conclusions can be drawn about the possibility of predicting viability on the basis of the smoothness of the surfaces evident during B-mode ultrasonography. Within the group with irregular bony ends, the 5 nonunion fractures with sharp ends typically had higher power Doppler scores and vessel counts than the 3 nonunion fractures with rounded ends. However, there was some overlap, making it difficult to assess the ability to predict vascularization by use of B-mode ultrasonography.

Types of nonunions have been divided into categories with more or less distinctive radiographic signs. The nonunions have been assumed to be avascular or vascular. However, it has been speculated[5] that even atrophic nonunions may be vascularized. This may even make it more difficult to radiographically predict the best surgical treatment. In the study reported here, there were vast differences in radiographic diagnoses among investigators, which indicated the difficulty of obtaining a correct prediction about vascularization of a nonunion fracture. When the mean radiographic predictions for the 6 investigators were compared with histologic results, a poor correlation with histologic vessel count was found. This would suggest that a radiographic assessment of the type of nonunion is insensitive.

When predicting vascularity by use of power Doppler ultrasonography, examination of the images suggested that the majority (6/8) of nonunion fractures were vascularized. The accuracy of this prediction was proven by the high correlation factors of the power Doppler variables, with results of histologic examination used as the criterion-referenced standard. Therefore, power Doppler ultrasonography is a useful tool for the assessment of vascularity of nonunion fractures prior to corrective surgery.

In another study,[15] no power Doppler ultrasonography signals were found at the fracture site in normally healing fractures 2 to 3 months after surgery. However, in the study reported here, vascularization was detected at the fracture site 3 to 12.5 months after surgery. This may indicate ongoing activity, and an option would have been to stabilize the vascularized nonunions without opening the fracture site. However, this was not investigated in our study.

Power Doppler ultrasonography was used in the study reported here, instead of color Doppler ultrasonography, because the objective was to verify blood vessels and blood flow and not the direction of blood flow. Power Doppler ultrasonography was chosen because it is more sensitive to flow and less dependent on the incident angle than is color Doppler ultrasonography.[17,18]

Use of software to measure regions of interest would have been a more objective method for measuring the surface areas of the Doppler signals. However, we chose to use a semiquantitative scoring system because this investigation was meant to be easily reproducible by clinicians. The cutoff points we used were arbitrarily chosen, but when we initially tested these ranges, we found that the scores obtained were comparable for the 3 categories. Also, we believed that not dividing the surface area into more categories (especially for the higher range of vessel area) was justified to compensate for the possibility of a cavitary lesion, a longitudinal image of a vessel, or several transsections of the same tortuous vessel. The high correlation between the histologic vessel count and our scoring system validated this method of scoring the nonunion fractures. However, surprisingly, the number of power Doppler signals had the same high correlation coefficient, so perhaps the mean number of power Doppler signals also may have yielded a good prediction. The vessel area had a poorer correlation, which may be explained by the fact that it was compared to the number of vessels counted during histologic examination, instead of comparing it to the vessel area per hpf.

The bone segment that contained 3 nonunion sites was obtained after amputation of the affected forelimb. The segment was decalcified prior to staining and immunolabelling. This differed from the processing of the surgically obtained samples of the other nonunion fractures. However, a similar amount of vascularization was evident on examination of H&E-stained and CD31-immunolabelled slides; therefore, the results for the 3 nonunion sites on the same affected forelimb were included in the study. A study[19] in which investigators assessed the influence of several decalcification procedures on immunoreactivity revealed that the staining intensity and number of positively stained cells were not significantly reduced, compared with results for nondecalcified control samples.

The vascularization of nonunion fractures found in the study reported here would lead to the speculation that obtaining rigid immobilization had priority over debridement and cancellous autograft placement. However, in all our surgically corrected fractures, treatment included placement of cancellous autografts, so no conclusions can be drawn from these results about the best surgical treatment for nonunions. Nonetheless, knowledge of the degree of vascularization may lead to more informed surgical planning. Because this study was performed on a relatively small group of nonunion fractures and all nonunion fractures were debrided and grafted, no recommendations can be made about the cutoff point for treatment of a nonunion fracture by use of stabilization and debridement or stabilization alone.

Another area in which results of the study reported here may be applied is delayed union fractures. Lack of vascularization in a delayed union fracture would suggest that the patient best be managed surgically, whereas a delayed union fracture with vascularized tissue at the fracture site may be a candidate for a more conservative approach. However, this has not been proven in a research or clinical setting.

The degree of vascularization as predicted by use of power Doppler ultrasonography had a good correlation with the number of vessels per hpf during histologic examination. This leads to the conclusion that atrophic nonunion fractures of dogs can be vascular and that power Doppler ultrasonography is a useful tool for assessing the vascularization in nonunion fractures. Radiographic prediction of vascularity proved to

be an insensitive tool. Knowledge of the viability of a nonunion fracture and the length of a nonviable segment obtained before corrective surgery can be used to help surgeons select the best treatment option.

a. HFG series A, Varian, Salt Lake City, Utah.
b. HF R105, Ralco, Milan, Italy, distributed by Verachtert equipment, Antwerp, Belgium.
c. GE Logiq 7, M12L (7 to 14 MHz), General Electrics, Milwaukee, Wis.
d. Aquasonic, Parker Laboratories Inc, Fairfield, NJ.
e. Monoclonal mouse anti-human CD31 clone JC70A, DakoCytomation, Glostrup, Denmark.
f. SAS, version 9.1, SAS Institute Inc, Cary, NC.

Appendix

Semiquantitative system used to score 3 categories of power Doppler ultrasonography signals. Each category was scored on a scale of 0 to 3.

Category	0	1	2	3
Color	No signal	Red or purple	Orange	Yellow
Vessel area (mm^2)	No signal	< 5	5–10	> 10
No. of vessels	No signal	< 5	5–10	> 10

References

1. Sumner-Smith G. Delayed unions and non-unions. Diagnosis, pathophysiology, and treatment. *Vet Clin North Am Small Anim Pract* 1991;21:745–760.

2. Millis DL, Jackson AM. Delayed unions, non-unions, and malunions. In: Slatter D, ed. *Textbook of small animal surgery*. 3rd ed. Philadelphia: WB Saunders Co, 2004;1849–1861.

3. Piermattei DL, Flo GL. Fractures: classification, diagnosis, and treatment. In: Piermattei DL, Flo GL, eds. *Brinker, Piermattei, and Flo's handbook of small animal orthopedics and fracture repair*. 3rd ed. Philadelphia: WB Saunders Co, 1997;24–146.

4. Toal RL. Fracture healing and complications. In: Thrall DE, ed. *Textbook of veterinary diagnostic radiology*. 3rd ed. Philadelphia: WB Saunders Co, 1998;142–159.

5. Brownlow HC, Reed A, Simpson AH. The vascularity of atrophic non-unions. *Injury* 2002;33:145–150.

6. Barros JW, Barbieri CH, Fernandes CD. Scintigraphic evaluation of tibial shaft fracture healing. *Injury* 2000;31:51–54.

7. Averill SM, Johnson AL, Chambers M, et al. Qualitative and quantitative scintigraphic imaging to predict fracture healing. *Vet Comp Orthop Traumatol* 2003;12:142–150.

8. Baltaxe HA, Shaw DD, Connolly JF. Assessment of healing of long-bone fractures by intraosseous venography. *Radiology* 1980;137:53–56.

9. Kuhlman JE, Fishman EK, Magid D, et al. Fracture nonunion: CT assessment with multiplanar reconstruction. *Radiology* 1988;167:483–488.

10. Tervonen O, Junila J, Ojala R. MR imaging in tibial shaft fractures. A potential method for early visualization of delayed union. *Acta Radiol* 1999;40:410–414.

11. Hannesschlager G, Reschauer R. Sonographic follow-up of secondary fracture healing. Initial experiences with morphologic and semiquantitative assessment of periosteal callus formation. *Rofo Fortschr Geb Rontgenstr Neuen Bildgeb Verfahr* 1990; 153:113–119.

12. Maffulli N, Thornton A. Ultrasonographic appearance of external callus in long-bone fractures. *Injury* 1995;26:5–12.

13. Herzog L, Huber FX, Meeder PJ, et al. Laser Doppler flow imaging of open lower leg fractures in an animal experimental model. *J Orthop Surg (Hong Kong)* 2002;10:114–119.

14. Caruso G, Lagalla R, Derchi L, et al. Monitoring of fracture calluses with color Doppler sonography. *J Clin Ultrasound* 2000;28:20–27.

15. Risselada M, Kramer M, van Bree H, et al. Power Doppler assessment of the neovascularization during uncomplicated fracture healing of long bones in dogs and cats. *Vet Radiol Ultrasound* 2006;47:301-307.

16. Risselada M, Kramer M, van Bree H. Approaches for ultrasonographic evaluation of long bones in the dog. *Vet Radiol Ultrasound* 2003;44:214–220.

17. Martinoli C, Derchi LE, Rizzatto G, et al. Power Doppler sonography: general principles, clinical applications, and future prospects. *Eur Radiol* 1998;8:1224–1235.

18. Nyland TG, Mattoon JS, Herrgesell EJ, et al. Physical principles, instrumentation, and safety of diagnostic ultrasound. In: Nyland TG, Mattoon JS, eds. *Small animal diagnostic ultrasound*. Philadelphia: WB Saunders Co, 2002;1–18.

19. Mukai K, Yoshimura S, Anzai M, et al. Effects of decalcification on immunoperoxidase staining. *Am J Surg Pathol* 1986;10:413–419.